Journal of Biomechanics 65 (2017) 106–114

Contents lists available at ScienceDirect

Journal of Biomechanics

journal homepage: www.elsevier.com/locate/jbiomech
www.JBiomech.com

Explosive lower limb extension mechanics: An on-land vs. in-water exploratory comparison

Brice Guignard [a,b,*], Jessy Lauer [a,b], Pierre Samozino [a], Luis Mourão [b,c,d], João Paulo Vilas-Boas [b,c], Annie Hélène Rouard [a]

[a] Inter-university Laboratory of Human Movement Science, Savoie Mont Blanc University, University Department SceM – Technolac, 73376 Le Bourget-du-Lac, France
[b] Porto Biomechanics Laboratory (LABIOMEP), University of Porto, Porto, Portugal
[c] Center of Research, Education, Innovation and Intervention in Sport, Faculty of Sport, University of Porto, Portugal
[d] Industrial and Management Studies Superior School, Porto Polytechnic Institute, Vila do Conde, Portugal

ARTICLE INFO

Article history:
Accepted 15 October 2017

Keywords:
Mechanical power
Force-velocity relationship
Aquatic environment
CFD
Squat jump

ABSTRACT

During a horizontal underwater push-off, performance is strongly limited by the presence of water, inducing resistances due to its dense and viscous nature. At the same time, aquatic environments offer a support to the swimmer with the hydrostatic buoyancy counteracting the effects of gravity. Squat jump is a vertical terrestrial push-off with a maximal lower limb extension limited by the gravity force, which attracts the body to the ground. Following this observation, we characterized the effects of environment (water vs. air) on the mechanical characteristics of the leg push-off. Underwater horizontal wall push-off and vertical on-land squat jumps of two local swimmers were evaluated with force plates, synchronized with a lateral camera. To better understand the resistances of the aquatic movement, a quasi-steady Computational Fluid Dynamics (CFD) analysis was performed. The force-, velocity- and power-time curves presented similarities in both environments corresponding to a proximo-distal joints organization. In water, swimmers developed a three-step explosive rise of force, which the first one mainly related to the initiation of body movement. Drag increase, which was observed from the beginning to the end of the push-off, related to the continuous increase of body velocity with high values of drag coefficient (C_D) and frontal areas before take-off. Specifically, with velocity, frontal area was the main drag component to explain inter-individual differences, suggesting that the streamlined position of the lower limbs is decisive to perform an efficient push-off. This study motivates future CFD simulations under more ecological, unsteady conditions.

1. Introduction

Water has a greater density and viscosity than air (water is fifty-five times more viscous than air at 20 °C, Denny (1993)), which impacts body equilibrium and displacement. Indeed, swimmers must (i) propel themselves in a horizontal position (typically, this is performed vertically on land), (ii) with the help of their four limbs (lower limbs on land) and (iii) in a moving environment offering both support and resistances (support is stable and rigid on land, and aerodynamics resistances are restricted). Consequently, swimming performance depends on the interaction of propulsive and resistive forces (Toussaint, 2002). Swimming differs from other popular sports since athletes' body translates horizontally to minimize water drag.

Race performance is positively correlated with the total time spent during the turns, depending on the race distance ($r = 0.80$–0.90; Arellano et al., 1994). According to Mason and Cossor (2001), the most relevant aspect of the turn performance is the *pushing-off the wall* action (i.e., a powerful extension of the lower limbs). Efficiency in this phase is determined by three essential components: an effective peak push-off force, an appropriate time spent in contact with the wall and a good streamlined position to limit the amount of drag during the push and the glide phase (Lyttle et al., 1998, 1999; Mason and Cossor, 2001). Classically, water drag was estimated from inverse dynamics approach,

* Corresponding author at: Inter-university Laboratory of Human Movement Science, Savoie Mont Blanc University, University Department SceM – Technolac, 73376 Le Bourget-du-Lac, France.
E-mail address: brice.guignard@neuf.fr (B. Guignard).

https://doi.org/10.1016/j.jbiomech.2017.10.024
0021-9290/

including wall push reaction forces and body Center of Mass (CM) acceleration, obtained by video recordings (Klauck, 2005; Lyttle et al., 1999). Such studies reported resultant drag (D) and effects of body velocity (v) without any information about drag coefficient (C_D) and frontal area (S), the two main parts of the drag largely affected by body position (Clarys, 1979). In consequence, the effects of drag parameters on the push-off performance were not explicitly characterized. Vilas-Boas et al. (2010) compared D, C_D and S values through inverse dynamics and planimetry in the two gliding positions of the breaststroke turn. Nevertheless, S was analyzed independently from the remaining two parameters.

Computational Fluid Dynamics (CFD) is a potent numerical tool to compute D, C_D and the instantaneous projected S (Bixler and Schloder, 1996). For instance, this analytical tool reinforced results of experimental approaches that investigated the impacts of accelerated movements through water to increase propulsive drag (i.e., estimation of drag and lift forces developed by a swimmer's hand in Bixler and Schloder, 1996). Moreover, CFD technique has the advantage of showing detailed characteristics of fluid flow around the swimmer's body (Marinho et al., 2011). Precisely, it may help evaluate the perturbations and turbulences in the behavior of water molecules (leading to *unsteady* flows; Gomes and Loss, 2015) following a swimmer's displacement in the aquatic environment. Because of the complexity of these ecological situations, simplifications are often made in numerical approaches to solve fluid flow equations, assuming a steady aquatic environment around the moving swimmer. In this way, previous CFD studies segmented a whole movement into *different successive positions*, to approach the fluid behavior in dynamical conditions. Using this strategy, Zaïdi et al. (2008) and Popa et al. (2014) characterized drag as a function of head position during gliding.

Powerful lower limb extensions are classically studied on land, where athletes perform this movement vertically, against their own body weight or with additional loads acting as resistances (Cormie et al., 2008). CM velocity, force development or thrust power are common variables measured to explain athletes' strategies when performing a vertical jump. Such movement is very close to the horizontal underwater wall push-off. More precisely, in water, the performance is strongly dependent on the body position (influencing both projected frontal area and drag coefficient) and fluid properties (e.g., depth in which the movement is performed and whether the fluid is in motion or not). On land, the body conformation and the distribution of masses act as performance-related parameters. Therefore, the main movement limitations that arise underwater are linked to *drag* (i.e., water is challenging the movement), while *gravity* mainly constrains the extension performed on land. By comparing the mechanical properties of both push-off, we sought to investigate the different *adaptive behaviors* a swimmer may develop to reach the task goal in the constraining aquatic environment. Consequently, kinetics and kinematics comparisons between a maximal lower limb extension performed in both conditions would provide additional insights into the impacts of aquatic constraints on lower limbs push-off strategy and hence, on performance. An underlying objective was to properly characterize the constraints of the underwater movement to develop swimmers' abilities in order to become efficient in the push-off sequence of a competitive turn. We hypothesized that resistive aquatic environment would prompt swimmers to reach lower take-off velocities (i.e., lower performance) in comparison to on-land condition. Additionally, to deeply examine the effects of aquatic constraints on the push-off mechanics, the different components of drag (v, C_D and S) will be investigated using a quasi-steady CFD approach.

2. Methods

2.1. Participants

Two male swimmers, volunteered to participate in this study [mean ± SD for age: 22 yr, height: 1.82 ± 0.03 m, and weight: 77.0 ± 2.8 kg]. They were previously informed about the experiment and signed a consent form approved by the local ethics committee. The limited number of participants involved in this study is due to the complexity of the CFD approach.

2.2. Experimental protocol

Swimmers performed two trials of maximal push-off against the wall, 0.8-m underneath the water surface to avoid significant wave drag (Vennell et al., 2006) and to reproduce ecological race conditions: arms extended over the head (shoulder flexed), hands joined and palms down. Then, swimmers performed two maximal on-land squat jumps with identical body configuration than during underwater push-off (Fig. 1). The replication of the body conformation consisted of measuring all joint angles of the lower limbs during the underwater push-off (Fig. 1), before reproducing it on land. Since no mobility measurements were performed, we asked swimmers to hold their arms firmly extended overhead (i.e., horizontally underwater and vertically on land). Analyses were conducted on each push-off yielding to the highest CM velocity.

2.3. Data collection

Five anatomical landmarks (humerus' greater tubercle, great trochanter, lateral condyle of the knee, lateral malleolus and head of the fifth metatarsal) were filmed during the underwater push-off by a digital video camera (Sony® HDR-CX160E 50 Hz, Tokyo, Japan), positioned 5-m sagittally, 0.8-m deep, in a waterproof housing (SONY Sports pack SPK-CXA, Tokyo, Japan). The video footage was calibrated using a 2-m rigid calibration perch with nine control points (20-cm spacing).

Reaction forces at swimmers' feet were recorded by two underwater extensometric force plates with a surface of 0.5 × 0.5-m, sensitivity of 2 N, error <1% and natural frequency of 60 Hz, mounted on a specially-built support fixed to the pool wall with a sampling frequency of 2000 Hz (de Jesus et al., 2013). Squat jump forces were registered by two force plates (Bertec Corporation, Columbus, OH, USA) with a surface of 0.6 × 0.9-m and sampling frequency of 400 Hz. Force plates were connected to an analogue-to-digital converter (National Instruments, NIcDAQ-9172). Underwater video footage and force signals were synchronized with a starter device (ProStart, Colorado Time Systems Corporation, Colorado, USA), which simultaneously produced a light signal to the video system and a trigger signal to the converter.

Three-dimensional virtual, realistic body models (with goggles and cap, Fig. 2) were created with Mephisto 3D full body scanner and software (Mephisto 3D, 4DDynamics, Antwerp, Belgium). The scan system had a texture resolution of 12.4 megapixels, and a point accuracy of 0.15 mm in average, creating 3D models composed of more than 70,000 cells. Swimmers' bodies were scanned in three different positions (beginning of the push-off, middle part, and position before take-off) to obtain a general overview of the drag history over the whole push: upper limbs extended above the head and lower limbs adopting a configuration similar to the one observed in water.

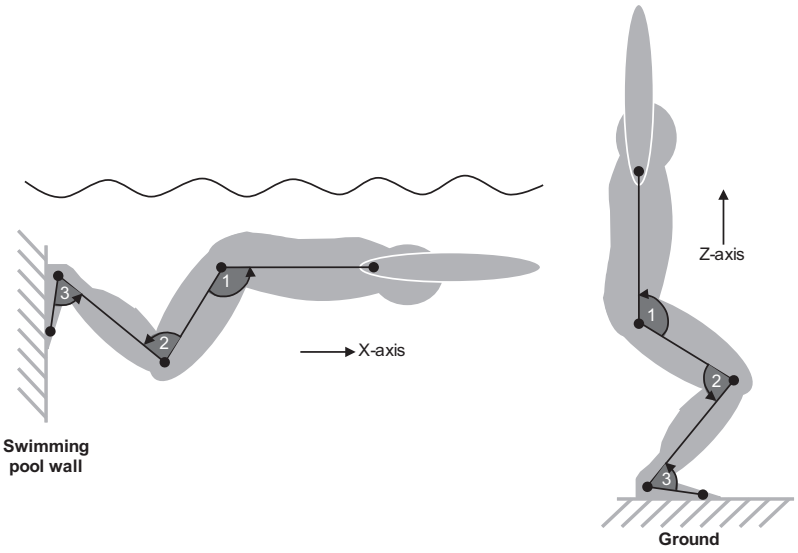

Fig. 1. Swimmer's body position during the underwater push-off (left panel) with the three measured angles in the sagittal plane (1: hip angle; 2: knee angle and 3: ankle angle) and during the on-land squat jump (right panel).

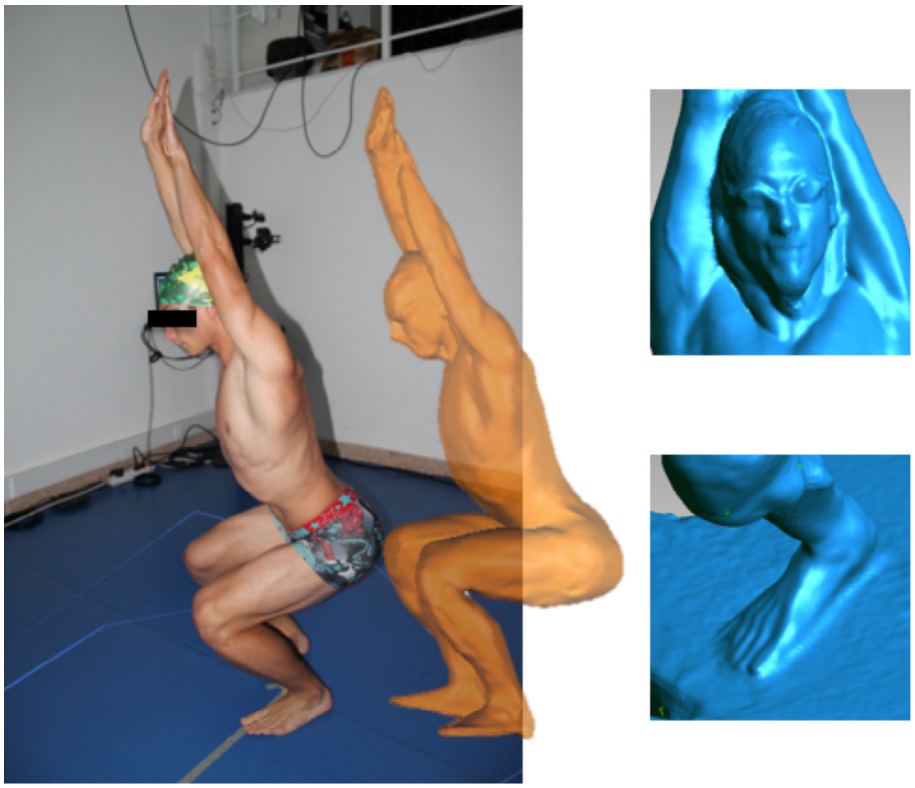

Fig. 2. Realistic body models obtained with Mephisto 3D scans (whole body and zooms on swimmer's head and foot).

2.4. Data treatment

2.4.1. Vertical on-land squat

CM vertical accelerations were computed using the Newton's second law of motion (a_Z in m/s^2). The CM vertical velocity (v_Z in m/s) is then obtained by trapezoidal integration of a_Z. Corresponding power (P_Z in W) was obtained by the product of the vertical component of the reaction force and the CM vertical velocity.

To quantify the swimmers' ability to rapidly produce high forces (i.e., athletes' explosiveness), the Rate of Force Development (RFD, in N/s) was computed as the ratio between the rise of force and the time to perform it (Aagaard et al., 2002).

2.4.2. Horizontal underwater push-off

The anatomical landmarks were digitized frame by frame (Matlab2013a, The MathWorks Inc., Natick, MA, USA; Fig. 3) to obtain the associated 2D coordinates (Hedrick, 2008). Force data were filtered through a fourth-order, low-pass (250 Hz) Butterworth filter. A notch filter was used in a second time to eliminate the 50 Hz frequency. The mass and the length of the upper body (head, torso

Fig. 3. Digitization software interface (upper panel) with position of anatomical landmarks in cyan dots. The accuracy of the digitization process is exemplified for the toes (red dot) on the left window. White dots symbolize CM trajectory throughout the push-off. Body positions, anatomical landmarks digitization and resulting CM positions during the maximal push-off are presented (lower panel). (For interpretation of the references to colour in this figure legend, the reader is referred to the web version of this article.)

Table 1
Boundary conditions and swimmers' model characteristics for the steady fluid flow CFD simulations.

	Characteristics
Three-dimensional domain	1.8-m deep, 2.5-m wide and 5.0-m long (Marinho et al., 2009); meshed with unstructured tetrahedral cells
Position of the swimmer model	At the center of the domain, 0.8-m deep
Number of cells in the domain	5.5 millions in average after the sensitivity study
Number of cells composing the swimming model	70,000 in average
Size of elements	0.5-m length (coarser far from boundaries) and 0.02-m length (finer in the vicinity of the body to better capture pressure gradients)
Water properties, flow and turbulence model	Steady and incompressible (Oertel et al., 2010): water density of 996.51 kg/m^3, temperature of 27 °C and kinematic viscosity of 0.856 * 10^{-6} m^2/s. v_X was swimmers' velocity at each selected positions. v_Z was 0. Outflow condition at the side behind the swimmer. k-ω turbulence model (best predictor of drag according to Zaïdi et al., 2010)

and upper limbs) and the lower limbs were then calculated (Shan and Bohn, 2003). The determination of the CM X-axis position was computed for each video frame (Fig. 3) according to tables of de Leva (1996).

CM velocity and acceleration were obtained from successive differentiation of CM position with respect to time. Push-off started when the CM forward velocity was superior to zero value and ended at take-off.

The instantaneous thrust power output (P_X in W) was computed as the product of the CM velocity (v_X in m/s) and the force (F_X in N).

From 2D coordinates, lower limb joint angles were determined in the sagittal plane. These angles determined the joints range of motion during the push-off and the positions computed with CFD.

2.4.3. Solving CFD equations, static conditions

Fluid flow analyses were performed using ANSYS® Fluent® Release 14.5 CFD software (ANSYS, Inc., Canonsburg, PA, USA). Boundary conditions of fluid flow and swimmers' model characteristics are presented in Table 1. This computational method was applied to study the three positions of the underwater push-off

to understand the effects of body conformation on the drag components for both subjects. To guarantee that the results were not affected by the resolution of the mesh, bodies of influence were created around the swimmers' models and their wake: inside these bodies, the mesh was made progressively finer until no change in hydrodynamic forces occurred.

The total drag (D) was obtained by the following Eq. (1) in each tested condition:

$$D = D_p + D_f \quad (1)$$

with D_p the pressure drag (N) and D_f the friction drag (N).

The drag coefficient (C_D) reflecting the hydrodynamic characteristics of the swimmer was determined using the following formula (2):

$$C_D = \frac{2 \cdot D}{\rho \cdot S \cdot v^2} \quad (2)$$

with ρ the water density (kg/m^3), S the area created by projecting the swimmer onto a perpendicular plane to the direction of flow (m^2) and v the steady free stream velocity of the water relative to the swimmer (m/s) (Bixler, 2008).

3. Results

Lower limb total extensions were completed in less than 500 ms for both subjects in water (498 for S1 and 469 ms for S2, Fig. 4), closed to on-land squat jump durations (523 for S1 and 456 ms for S2).

For both conditions, force patterns (Fig. 4a) were characterized by similar asymmetric bell profiles reaching concomitant peak values for S2 and 13% lower underwater for S1. In water, the rise of force presented three steps: a steep increase from 0 to 10 N/kg (0–200 ms) followed by a pseudo steady-state level of force (200–320 ms) ending by a second strong increase of force, from 10 to 20 N/kg (320–400 ms). On land, the force increased slightly from the push initiation to 180 ms for S1 and 240 ms for S2, followed by a slight decrease before a second rise of force, leading to peak values (around 450 ms for S1 and 360 ms for S2).

Despite similar peak values, the RFD registered underwater (3705.8 N/s for S1 and 3973.7 N/s for S2) was about twice as much as that observed on land (1983.7 N/s and 2179.0 N/s), with greater force range for water (from zero to maximal value) compared to on land (from body weight to maximal value; Fig. 4b). This conducted to great differences for mean values, 48% lower during water (604.2 and 585.6 N, i.e., 7.6 and 7.8 N/kg, respectively for S1 and S2) than on land (1143 and 1116 N, i.e., 14.5 and 14.9 N/kg).

Velocity-time relationships (Fig. 4c) followed curvilinear patterns in both environments. Mean velocities were close (0.97 m/s for S1 and 1.04 m/s for S2 (water), 1.06 m/s and 1.06 m/s (on land)) with higher take-off velocities in water than on land for S2 (3.06 m/s (water) and 2.54 m/s (on land)).

Thrust power-time curves (Fig. 4d) presented a similar tendency as the force profile. Water maximal power was lower (2556 and 3137 W for S1 and S2) than on land (3750 W and 3440 W, respectively). Mean power was 32% lower in water (802.2 and 869.8 W for S1 and S2) in comparison to 1250 and 1205 W on land.

From a kinematical viewpoint, the beginning of the aquatic push-off started by hip extensions for both subjects. The knee angle remained stable during the first part of the push, followed by a strong extension starting around 200 ms for S1 and 180 ms for S2, concomitant to the first rise of force. The ankle joint extended after 400 ms for S1 and 350 ms for S2, corresponding to a second rise of force (Fig. 5).

The CFD resolution study inside the bodies of influence led to a selection of 5.5 million tetrahedron elements to mesh the domain. This was the best compromise between simulation accuracy and the demand for computational power (an increase of this number resulted to no significant modifications of drag values). Angular values of the lower limb joints used in the CFD simulations are presented in Table 2. S increased for S1 throughout the movement, while it slightly decreased for S2 over the same period (Fig. 6). C_D presented relative stable values in the two first positions for both subjects with lower values for S1. Conversely, position before take-off was characterized by a higher increase of C_D for S1 and a strong decrease for S2. The D increased over the three studied positions similarly to CM velocity.

4. Discussion

The aim of the present study was to analyze the impacts of aquatic constraints on lower limbs push-off strategy (i.e., on performance) and reveal swimmers' adaptability to aquatic environment in comparison to a similar leg extension performed vertically on land.

Similarities were observed in both environments for the explosive lower limb extension mechanics. First, push-off durations were in the same order than previous values referenced for on-land squat jumps (Bobbert and Casius, 2005), and underwater horizontal push-off (Daniel et al., 2003; Takahashi et al., 1983). Each push-off was performed with successive extensions of hip, knee and ankle, indicating a *proximo-distal* sequence, already described for on-land vertical jumps (Haguenauer et al., 2005; van Ingen Schenau, 1989). This proximo-distal coordination is efficient to transmit forces and power to distal structures to complete a jump (van Ingen Schenau, 1989). Force-, velocity-, and power-time patterns were similar in water and on land, with asymmetric bell force-time patterns. This result is congruent with the conclusions made in previous on-land (Cormie et al., 2008; Samozino et al., 2008) and swimming turns studies (Roesler, 2003). Also, maximal force values remained in the same range in both environments. These observations highlighted that the general push-off mechanics are comparable in water vs. on-land, despite strong differences in body orientation and environmental constraints. Similar conclusions were obtained by Aerts and Nauwelaerts (2009) on batrachians push for both jumping and swimming. The authors concluded that the motor control strategy for generating propulsive impulses in each condition is quite equivalent. The results of our study seemed to demonstrate that the effect of water drag in horizontal position mimics the effect of gravity in on-land vertical squat (i.e., the swimmers are adapted to aquatic constraints by replicating the general characteristics of the movement performed on land), in spite of our small size sample.

The general shape of the velocity-time relationships observed in water was reproduced on land (e.g., mean velocities around 1 m/s in all tested conditions, confirming previous unloaded squat jump results; Cormie et al., 2008; Cuk et al., 2014). Unexpectedly, take-off velocities were *slightly* higher underwater than on land. To investigate this phenomenon, additional Electromyographic (EMG) measurements would be necessary to better characterize swimmers' muscular capabilities.

Due to lower general force values underwater and similar profiles of velocity, the power productions were consequently lower underwater in comparison to on-land push-off (i.e., power was computed as the product of the CM velocity and the force). This was quantified using RFD computations (i.e., individual explosiveness; Aagaard et al., 2002), with underwater values twice as on-land, despite similar force peaks in both environments. Such low RFD values are linked to gravity determining the initial force level

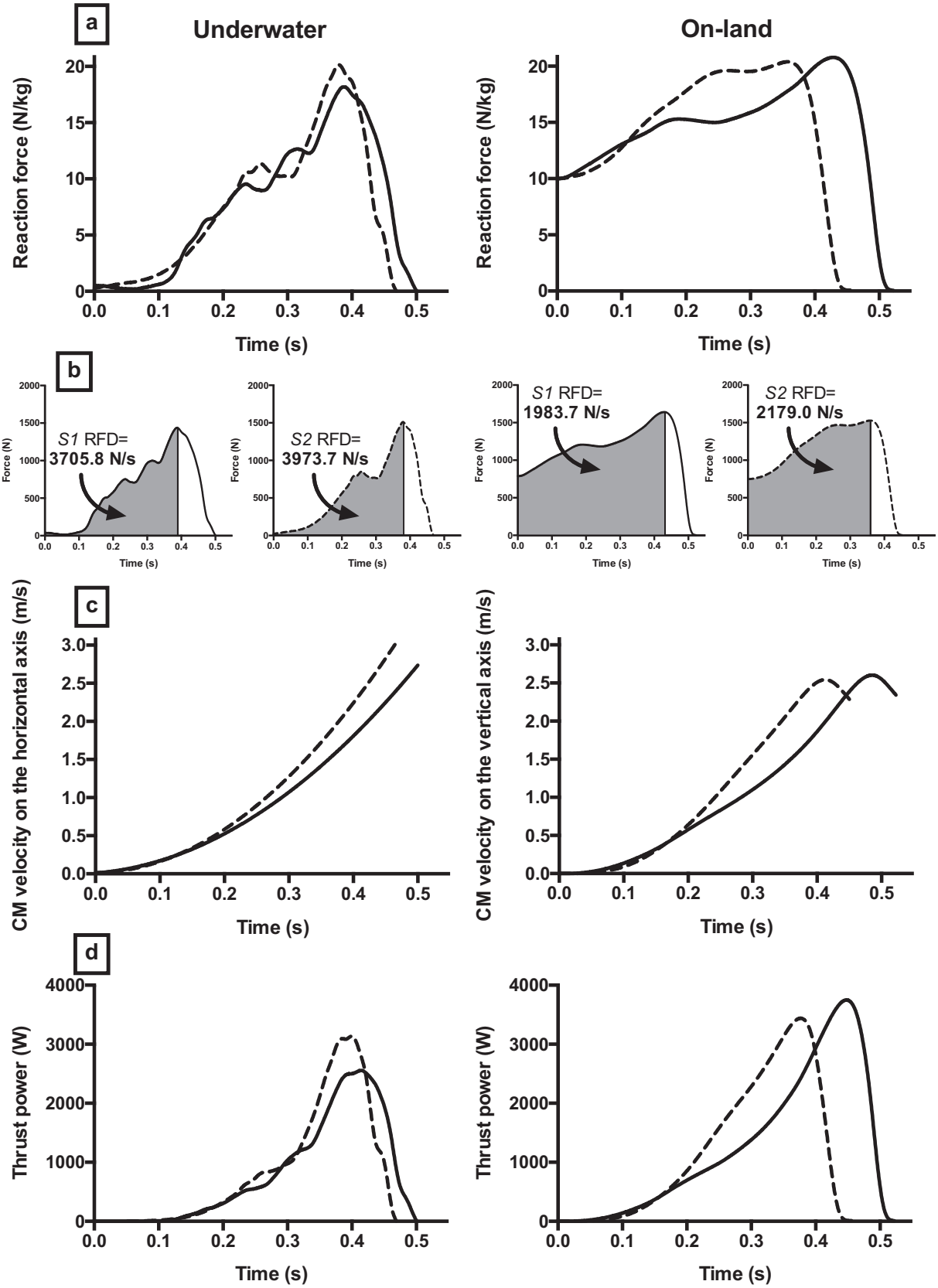

Fig. 4. Reaction forces (a), RFD (b), CM velocities (c) and thrust power (d) developed by Subject 1 (in continuous line) and Subject 2 (in dashed line) during the horizontal underwater push-off and the vertical on-land squat.

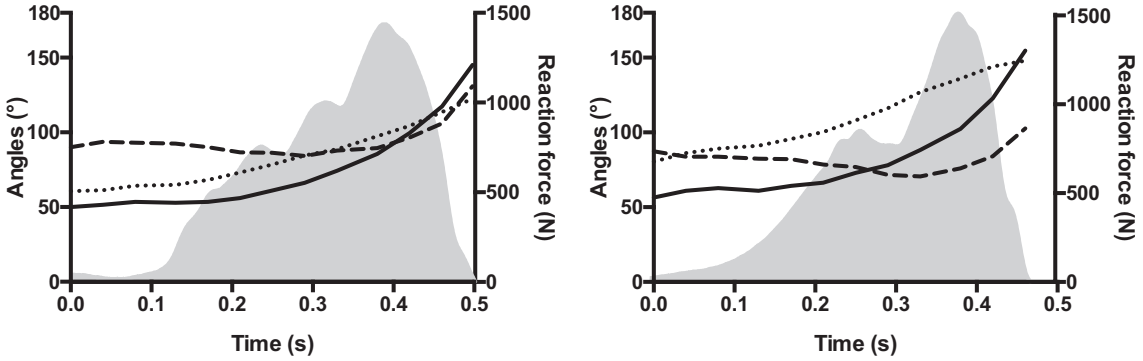

Fig. 5. Angles of the hip (dot line), the knee (continuous line) and the ankle (dash line) in the sagittal plane for Subject 1 (left panel) and Subject 2 (right panel) during the underwater push-off. The corresponding force developed by each subject was represented in grey.

Table 2
Lower limb angles (in degree) for both subjects for the three positions computed by CFD.

Position	Beginning		Middle		Take-off	
	S1 (°)	S2 (°)	S1 (°)	S2 (°)	S1 (°)	S2 (°)
Hip angle	64.8	89.1	84.5	108.1	113.7	148
Knee angle	52.9	62.7	66.2	73	117.4	154.7
Ankle angle	92.4	83.8	84.2	76.9	106.1	102.7

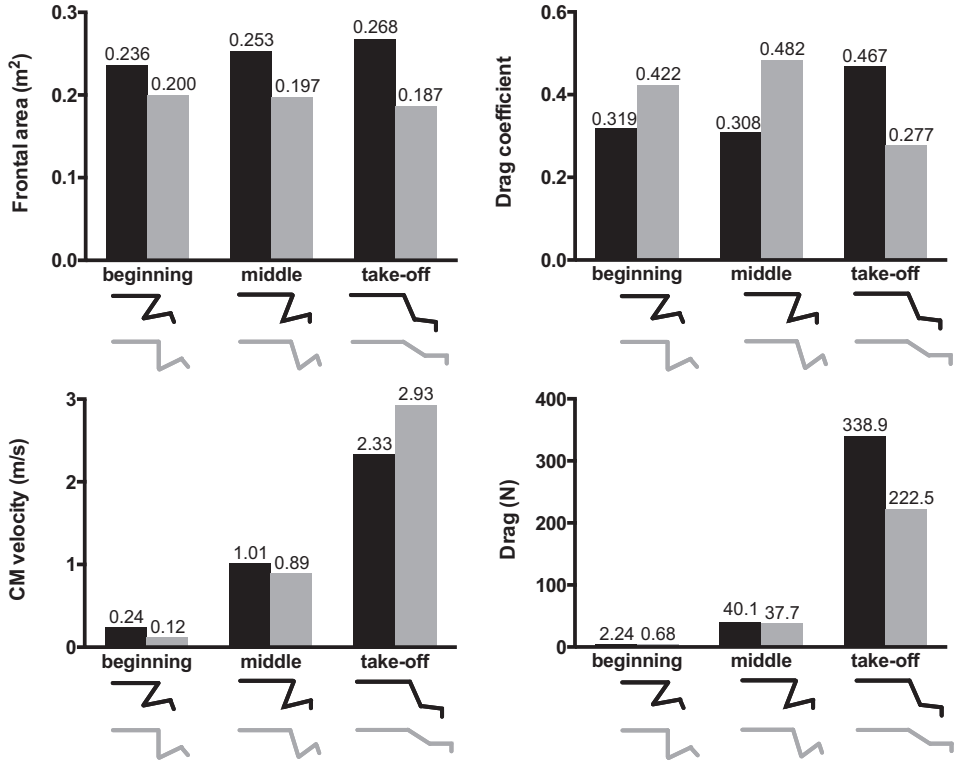

Fig. 6. Frontal area, C_D, CM velocity (antero-posterior axis) and drag for the three positions of the push (beginning, middle, take-off: sticks under the histograms) and the two participants (Subject 1 in black; 2 in grey).

(the heavier the swimmer is, the higher the initial force value is recorded). Furthermore, the rises of force differed with a three-step increase in water, the first one (from 0 to 10 N/kg) corresponding to the time necessary to initiate full body movement, and ending with a value equivalent to the one observed at the beginning of the on-land push. During the second step, the force presented a pseudo steady-state that appeared as a transition phase and during the third step, an important increase of force characterized the effectiveness of the push-off. Finally, RFD values revealed that the push-off movement is more explosive in water. This might be linked to the complexity of initiating body movement in water at the beginning of the push-off (i.e., defined as an impulsive start with low angle of attack according to Dickinson, 1996). Underwater, the environment acts as a supplementary load

compared to body movement initiation on land. Similarities have been described by Cormie et al. (2008) during on-land squat jumps: the authors concluded that the heavier the load carried, the steeper the rise of force, hence, the lower peak of thrust power.

Although the two movements performed on land and underwater demonstrated similar push-off mechanics, some of these results attested to *individual adaptations*. For instance, S1 was able to produce only 87% of the force peak developed on land, whereas S2 can approximately maintain his force peak in both environments. S1 seems to be more influenced by water drag, as demonstrated by lower force peaks and thrust power (P_X 32% lower in water).

The characterization of inter-individual differences – firstly highlighted by a biomechanical investigation – should be reinforced by the use of a quasi-steady CFD analysis. These investigations were carried out to thoroughly examine the relative importance of the different factors (v and S) that influence the total drag and the drag coefficient to perform the underwater push-off, and hence to study propulsion strategies of both swimmers. Drag remained low at the first analyzed position and then increased throughout the push-off, confirming previous observations (Clarys, 1979). Without the possibility to demonstrate the classical *quadratic* dependence of drag on velocity (restricted number of analyzed positions), our results highlighted that drag progression is strongly related to velocity increase (Toussaint et al., 1988). However, inter-individual discrepancies could not be exclusively linked to velocity dynamics, since S1 presented higher drag peak (340 N) than S2 (220 N) for a lower velocity peak (2.73 vs. 3.06 m/s). Despite slight modifications of S from first to third positions (increase of 13.5% for S1 and slight decrease of 6.5% for S2), this parameter seems to play an important role before take-off (0.268 m^2 for S1 vs. 0.187 m^2 for S2). Interestingly, the way swimmers minimize drag at the highest velocities is mainly related to their capacity to reduce S, appearing as a strong determinant of performance. Similarly, swimmers' hydrodynamic characteristics (assessed by the C_D) support that S1 undergone higher resistances in the last position with a C_D 68% higher compared to S2 at that moment. These results indicated that for high velocities, the inter-individual D differences are more related to S than to v, corroborating previous investigations. Indeed, D and S relationship was already demonstrated during glide analyses, since different head positions (i.e., different projected swimmers' frontal area) may significantly increase drag values. In 2D, Zaïdi et al. (2008) demonstrated that a head lowered instead of being aligned with the body increased drag about 17 up to 21%, at important speeds (2.2 up to 3.1 m/s). This was confirmed in 3D by Popa et al. (2014), who found that the aligned head position offered less resistance than lifted up and lowered head positions (head position accounted for 4% of total drag increase, whatever the swimmer's speed). In our study, verbal instructions were given to the swimmers in order to maintain the same upper limbs position throughout the push-offs. In this sense, even though slight modifications of upper body conformation may appear (the mobility of this body portion was not quantified), S differences should be related mainly to the lower limbs position, highlighting their major implication in the resistance process. An interesting paradox is that swimmers have to deal with an increase of v to maximize performance (negative effect with D increase) and a decrease of S (D reduction) to prepare the body to leave the wall in a streamlined position (Lyttle et al., 1999). S1 presented difficulties to adopt such a strategy since he started the movement with the lower limbs strongly bent under the trunk: his hip angle was 64.8° and his knee angle was 52.9°. In this configuration, shanks and feet are not fully aligned with the rest of the body, leading to a greater S and consequently D. The large range of motion corresponding to hip and knee full extension is not completed at the third position, explaining higher values of D for S1 (i.e., important S = 0.268 m^2). On the contrary, S2 adopted larger hip and knee openings at that moment (148 and 154.7°, respectively), allowing him to align his lower limbs with the upper body. Indeed, S2 C_D value at the third position (0.277) indicates a streamlined body position, already observed during free gliding, at a hypothetical velocity of 3 m/s (Marinho et al., 2009). Consequently, the greater water drag effect observed for S1—conducting to lower velocity-time productions—seemed mainly related to the worst body position *at the end* of the push-off. These results strongly suggested the importance of individualized analyses of hydrodynamic constraints during high power performances, but also reinforce the relevance of adopting a streamlined position before take-off in order to minimize D and consequently optimize performance (Butcher et al., 2007; Zamparo et al., 2009).

Nevertheless, these exploratory results are limited since CFD simulations were conducted under quasi-static flow conditions. Future investigations should incorporate whole body accelerations in the numerical model to better predict amounts of resistive forces faced by the swimmer (Rouboa et al., 2006). According to Caspersen et al. (2010), we can legitimately consider that present results underestimate from 25% drag values and its determinants compared to real unsteady conditions.

5. Conclusions

Despite high aquatic resistances, the general shape of the push-off mechanics were similar for underwater vs. on land push-off, demonstrating swimmers' adaptability. The performance (i.e., speed at take-off) was even slightly higher underwater, indicating that the two swimmers who participated in this study were possibly less affected by density and viscosity underwater than by gravity on land. Differences appeared on the way the force is produced, especially at movement initiation. Therefore, aquatic environment propulsive strategy remained more complex than a similar movement performed on land.

CFD results highlighted the main contribution of swimmers' frontal area (related to body segments positions) to determine drag at push-off higher velocities. Indeed, with velocity, frontal area was the main drag component explaining inter-individual differences, suggesting that a lower limbs streamlined position is the most adaptive behavior to perform an efficient push-off. Such results, connected with previous CFD investigations, revealed the importance of using numerical investigations based on realistic body geometries to discriminate the effects of limbs position on the performance.

Coaches and swimmers may use these results to enhance swimming turns efficiency, limiting hip and knee flexion at push initiation and performing a quick hip opening to adopt early the most streamlined position before take-off. These findings could also help coaches to consider new on-land training sessions to maximize the performance of their athletes during turns in swimming.

Nevertheless, this exploratory approach has to be completed by further investigations (larger sample of swimmers, unsteady and full dynamic flow analyses). Therefore, this quasi-steady study constitutes a first and original step to better understand the effects of different components of water constraints on push-off biomechanics.

Conflict of interest

The authors declare no conflict of interest.

References

Aagaard, P., Simonsen, E.B., Andersen, J.L., Magnusson, P., Dyhre-Poulsen, P., 2002. Increased rate of force development and neural drive of human skeletal muscle following resistance training. J. Appl. Physiol. 93, 1318–1326.

Aerts, P., Nauwelaerts, S., 2009. Environmentally induced mechanical feedback in locomotion: frog performance as a model. J. Theor. Biol. 261, 372–378.

Arellano, R., Brown, P., Cappaert, J., Nelson, R.C., 1994. Analysis of 50-, 100-, and 200-m freestyle swimmers at the 1992 Olympic Games. J. Appl. Biomech. 10, 189–199.

Bixler, B., 2008. The mechanics of swimming. In: Stager, J.M., Tanner, D.A. (Eds.), Handbook of Sports Medicine and Science, Swimming. Blackwell Science, Oxford, pp. 51–58.

Bixler, B., Schloder, M., 1996. Computational fluid dynamics: an analytical tool for the 21st century swimming scientist. J. Swim. Res. 11, 4–22.

Bobbert, M.F., Casius, L.J.R., 2005. Is the effect of a countermovement on jump height due to active state development? Med. Sci. Sports Exerc. 37, 440–446.

Butcher, S.J., Craven, B.R., Chilibeck, P.D., Spink, K.S., Grona, S.L., Sprigings, E.J., 2007. The effect of trunk stability training on vertical takeoff velocity. J. Orthop. Sports Phys. Ther. 37, 223–231.

Caspersen, C., Berthelsen, P.A., Eik, M., Pâkozdi, C., Kjendlie, P.-L., 2010. Added mass in human swimmers: age and gender differences. J. Biomech. 43, 2369–2373.

Clarys, J.P., 1979. Human morphology and hydrodynamics. In: Terauds, J., Bedingfield, E.W. (Eds.), Swimming III. University Park Press, Baltimore, pp. 3–41.

Cormie, P., McBride, J.M., McCaulley, G.O., 2008. Power-time, force-time, and velocity-time curve analysis during the jump squat: impact of load. J. Appl. Biomech. 24, 112–120.

Cuk, I., Markovic, M., Nedeljkovic, A., Ugarkovic, D., Kukolj, M., Jaric, S., 2014. Force-velocity relationship of leg extensors obtained from loaded and unloaded vertical jumps. Eur. J. Appl. Physiol. 114, 1703–1714.

Daniel, K., Klauck, J., Bieder, A., 2003. Kinematic and dynamographic research in different swimming turns. In: Proceedings of the 9th World Symposium of Biomechanics and Medicine in Swimming. University of Saint Etienne, Saint Etienne.

de Jesus, K., de Jesus, K., Figueiredo, P., Gonçalves, P., Pereira, S.M., Vilas-Boas, J.-P., Fernandes, R.J., 2013. Backstroke start kinematic and kinetic changes due to different feet positioning. J. Sports Sci. 31, 1665–1675.

de Leva, P., 1996. Adjustments to Zatsiorsky-Seluyanov's segment inertia parameters. J. Biomech. 29, 1223–1230.

Denny, M.W., 1993. Air and Water: The Biology and Physics of Life's Media. Princeton University Press, Princeton.

Dickinson, M.H., 1996. Unsteady mechanisms of force generation in aquatic and aerial locomotion. Am. Zool. 36, 537–554.

Gomes, L.E., Loss, J.F., 2015. Effects of unsteady conditions on propulsion generated by the hand's motion in swimming: a systematic review. J. Sports Sci. 33, 1641–1648.

Haguenauer, M., Legreneur, P., Monteil, K.M., 2005. Vertical jumping reorganization with aging: a kinematic comparison between young and elderly men. J. Appl. Biomech. 21, 236–246.

Hedrick, T.L., 2008. Software techniques for two- and three-dimensional kinematic measurements of biological and biomimetic systems. Bioinspirat. Biomimet. 3, 034001–034006.

Klauck, J., 2005. Push-off forces vs kinematics in swimming turns: model based estimates of time-dependent variables. Hum. Movem. 6, 112–115.

Lyttle, A.D., Blanksby, B.A., Elliott, B.C., 1998. Optimising kinetics in the freestyle flip turn push-off. In: Proceedings of the 16th International Symposium of Biomechanics in Sports. University of Konstanz, Germany.

Lyttle, A.D., Blanksby, B.A., Elliott, B.C., Lloyd, D.G., 1999. Investigating kinetics in the freestyle flip turn push-off. J. Appl. Biomech. 15, 242–252.

Marinho, D.A., Reis, V.M., Alves, F.B., Vilas-Boas, J.-P., Machado, L., Silva, A.J., Rouboa, A.I., 2009. Hydrodynamic drag during gliding in swimming. J. Appl. Biomech. 25, 253–257.

Marinho, D.A., Silva, A.J., Reis, V.M., Barbosa, T.M., Vilas-Boas, J.-P., Alves, F.B., Machado, L., Rouboa, A.I., 2011. Three-dimensional CFD analysis of the hand and forearm in swimming. J. Appl. Biomech. 27, 74–80.

Mason, B.R., Cossor, J.M., 2001. Swim turn performances at the Sydney 2000 Olympic Games. In: Proceedings of the 19th International Symposium of Biomechanics in Sports. University of San Francisco, San Francisco.

Oertel, H., 2010. Prandtl-Essentials of Fluid Mechanics. Springer, New York.

Popa, C.V., Arfaoui, A., Fohanno, S., Taïar, R., Polidori, G., 2014. Influence of a postural change of the swimmer's head in hydrodynamic performances using 3D CFD. Comput. Methods Biomech. Biomed. Eng. 17, 344–351.

Roesler, H., 2003. Turning force measurement in swimming using underwater force platforms. In: Proceedings of the 9th World Symposium of Biomechanics and Medicine in Swimming. University of Saint Etienne, Saint Etienne.

Rouboa, A.I., Silva, A.J., Leal, L., Rocha, J., Alves, F.B., 2006. The effect of swimmer's hand/forearm acceleration on propulsive forces generation using computational fluid dynamics. J. Biomech. 39, 1239–1248.

Samozino, P., Morin, J.B., Hintzy, F., Belli, A., 2008. A simple method for measuring force, velocity and power output during squat jump. J. Biomech. 41, 2940–2945.

Shan, G., Bohn, C., 2003. Anthropometrical data and coefficients of regression related to gender and race. Appl. Ergon. 34, 327–337.

Takahashi, G., Yoshida, A., Tsubakimoto, S., Miyashita, M., 1983. Propulsive forces generated by swimmers during a turning motion. In: Hollander, A.P., Huiging, P. A., de Groot, G. (Eds.), Biomechanics and Medicine in Swimming. Human Kinetics Publisher, Champaign, pp. 192–198.

Toussaint, H.M., 2002. Biomechanics of propulsion and drag in front crawl swimming. In: Proceedings of the 10th International Symposium on Biomechanics in Sports. University of Extremadura, Cáceres.

Toussaint, H.M., de Groot, G., Savelberg, H.H.C.M., Vervoorn, K., Hollander, A.P., van Ingen Schenau, G.J., 1988. Active drag related to velocity in male and female swimmers. J. Biomech. 21, 435–438.

van Ingen Schenau, G.J., 1989. From rotation to translation: constraints on multi-joint movements and the unique action of bi-articular muscles. Hum. Mov. Sci. 8, 301–337.

Vennell, R., Pease, D., Wilson, B., 2006. Wave drag on human swimmers. J. Biomech. 39, 664–671.

Vilas-Boas, J.-P., Costa, L., Fernandes, R., Ribeiro, J., Figueiredo, P., Marinho, D., Silva, A., Rouboa, A., Machado, L., 2010. Determination of the drag coefficient during the first and second gliding positions of the breaststroke underwater stroke. J. Appl. Biomech. 26, 324–331.

Zaïdi, H., Fohanno, S., Taïar, R., Polidori, G., 2010. Turbulence model choice for the calculation of drag forces when using the CFD method. J. Biomech. 43, 405–411.

Zaïdi, H., Taïar, R., Fohanno, S., Polidori, G., 2008. Analysis of the effect of swimmer's head position on swimming performance using computational fluid dynamics. J. Biomech. 41, 1350–1358.

Zamparo, P., Gatta, G., Pendergast, D.R., Capelli, C., 2009. Active and passive drag: the role of trunk incline. Eur. J. Appl. Physiol. 106, 195–205.